Proc. Natl. Acad. Sci. USA
Vol. 81, pp. 488–492, January 1984
Developmental Biology

Amounts, synthesis, and some properties of intracisternal A particle-related RNA in early mouse embryos

(endogenous retrovirus/gene expression/early development/RNA·DNA hybridization)

LAJOS PIKÓ*†, MICHELE D. HAMMONS*, AND KENT D. TAYLOR*

*Developmental Biology Laboratory, Veterans Administration Medical Center, Sepulveda, CA 91343; and †Division of Biology, California Institute of Technology, Pasadena, CA 91125

Communicated by Roy J. Britten, September 30, 1983

ABSTRACT **Early mouse embryos express two morphological subtypes of intracisternal A-type particles, one resembling those occurring in mouse tumors (referred to as IAP) and the other apparently specific for early embryos [referred to as IAP(ε)]. Using cloned fragments of IAP genes as labeled probes in dot-hybridization experiments, we detected IAP-related RNA sequences in mouse oocytes and preimplantation embryos. IAP RNA is relatively abundant in ovarian oocytes, is reduced in amount to ≈1/10th in the ovulated egg, and increases ≈100 times (from ≈1.3 × 10^3 to ≈1.5 × 10^5 molecules per embryo) between the one-cell stage and late blastocyst stage. Most of the IAP RNA consists of a single size class of about 5.4 kilobases, and a major fraction of this RNA is polyadenylylated. Quantitative considerations suggest that only a few percent of the IAP RNA in embryos are associated with particles. In two-cell embryos, the number of IAP RNA molecules is <1/10th the number of IAP(ε) particles, suggesting that IAP(ε) is genetically distinct from IAP and presumably represents a family of as yet unidentified retrovirus-like elements.**

Early mouse embryos regularly express several types of virus-like structures whose appearance is correlated with specific stages of development (for review, see refs. 1 and 2). Intracisternal A-type particles (IAPs), of which two morphological subtypes have been distinguished (3, 4), are the most prominent. Particles of one subtype, termed "small A particles" (3) or, more recently, "ε-particles" to emphasize their distinctness (4), seem to be specific for early embryonic cells and form in large clusters in two- to eight-cell embryos but are absent or sparse at other stages (3–7). We will refer to these particles as IAP(ε)s. The other subtype, designated "large A particles" by Chase and Pikó (3), is morphologically very similar to the IAPs that are abundant in many mouse tumors including myelomas (8). Large A particles are present in ovarian oocytes until ovulation, are rarely seen in the ovulated egg and early cleavage-stage embryos, but increase in number from the eight-cell stage onwards through the blastocyst (3, 4). In this report, we will restrict the term IAP to this second type of A particle. The role of either subtype of A particle in embryo development is unclear at present, but there is evidence for the cell-surface expression of IAP-related antigens in early embryonic cells (9, 10).

The IAPs found in tumor cells have many properties resembling those of infectious retroviruses, but IAPs are genetically distinct from the mouse type B and type C viruses (11, 12). IAPs have reverse transcriptase activity (13) and contain polyadenylylated RNA of 3.5 to 7 kilobases (kb) (14, 15), which codes for the major particle protein p73 (14). There are ≈1,000 IAP genes (provirus-like genetic elements) per haploid mouse genome (15–17), and genomic clones of several of these have been isolated and analyzed (15, 18, 19). The predominant gene form is 7 kb in length (18, 19), but shorter units with major deletions and substitutions also have been found (15, 17). IAP genes are bordered by direct long terminal repeats (LTRs) of about 0.35 kb, which are similar in structure to the proviral LTRs of infectious retroviruses (20, 21). IAP gene insertions were found in two mutant mouse κ light-chain genes (21) and in a cellular oncogene (22), suggesting that IAP elements may be a significant source of genetic variability in mice.

In the present work, we used cloned IAP DNA probes to detect and analyze the IAP-related RNA sequences in mouse oocytes and early embryos.

MATERIALS AND METHODS

Oocytes and Embryos. $CD2F_1$ (BALB/c♀ × DBA/2♂; Simonsen Laboratories, Gilroy, CA) prepubertal female mice were induced to superovulate and mated to $CD2F_1$ males. Unfertilized eggs (freed of follicle cells) and embryos up to the early blastocyst (32 cells) stage were collected directly from the oviducts; expanded blastocysts (64 cells) were obtained by culturing early blastocysts overnight (23). Growing and fully grown oocytes were isolated by the procedure of Eppig (24).

Extraction of RNA. Batches of embryos were digested with 0.5% $NaDodSO_4$ containing 100 μg of proteinase K per ml, and the RNA was extracted with phenol/chloroform in the presence of *Escherichia coli* tRNA carrier as described (25). Unlabeled embryo lysates also contained about 1 ng of [^{3}H]cRNA made to λ phage DNA (26) (specific activity, 2.5 × 10^7 cpm/μg) as an internal recovery marker. An RNA standard containing IAP RNA was prepared from a post-membrane supernatant fraction (10,000 × *g* for 20 min) (27) of a homogenate of MOPC-104E myeloma maintained in BALB/c mice by subcutaneous passage. The high molecular weight RNA in this fraction was precipitated and washed extensively with 2 M LiCl (28). For use in dot hybridization, embryo and standard RNAs were digested with 20 μg of DNase I (RNase-free, Worthington) per ml of 0.1 M NaCl/10 mM Tris·HCl, pH 7.5/5 mM $MgCl_2$ at 37°C for 15 min.

Recombinant DNA Clones. Recombinant λ phage clones carrying IAP gene sequences were selected from a mouse genomic library. BALB/c sperm DNA fragments of 12–20 kb were isolated after partial digestion with the restriction enzymes *Hae* III/*Alu* I and inserted into λ phage Charon 4A by means of *Eco*RI linkers (29). (We are indebted to Mark Davis and Lee Hood for making this library available to us.) Poly(A)$^+$ RNA was isolated from gradient-purified IAP from the mouse myeloma line MOPC-104E and transcribed into ^{32}P-labeled cDNA as described by Lueders *et al.* (27) except

The publication costs of this article were defrayed in part by page charge payment. This article must therefore be hereby marked "*advertisement*" in accordance with 18 U.S.C. §1734 solely to indicate this fact.

Abbreviations: IAP, intracisternal A particle of the type occurring in mouse tumor cells; IAP(ε), intracisternal A particle of the type occurring in early mouse embryos; LTR, long terminal repeat; kb, kilobase(s).

for the use of calf thymus DNA fragments as primer. This cDNA was used to screen (30) $\approx 10^4$ plaques on *E. coli* DP50SupF, yielding ≈100 reactive clones, and to analyze the DNA of reactive clones by Southern blot hybridization (31). Of 20 clones selected at random, 10 were found to contain complete copies or large segments of IAP genes, and these were examined in greater detail as to restriction-site pattern and sequence homology of heteroduplexes. Specific IAP gene fragments were subcloned into the single-stranded DNA phage M13mp8 (32) or the plasmid pUC8 (33) for use as hybridization probes. M13 vectors, pUC plasmids, and host cells *E. coli* JM103 and JM83 were obtained from Bethesda Research Laboratories.

Labeled DNA Probes. Single-stranded M13 phage DNA carrying the appropriate inserts was isolated by precipitation of the phage with polyethylene glycol and extraction with phenol/chloroform (34). By using a 17-nucleotide primer (P-L Biochemicals) complementary to the region 5′ to the multiple cloning site, a duplex segment ≈1.5 kb long was synthesized (35) with the Klenow fragment of *E. coli* DNA polymerase (Bethesda Research Laboratories). [α-^{32}P]dTTP was added to the reaction mixture to give a specific activity of $\approx 1\text{–}2 \times 10^8$ dpm/μg of recombinant DNA (M13 DNA plus insert). A ^{32}P-labeled single-stranded DNA tracer complementary to IAP RNA was prepared by using the 1.4-kb *Bam*HI fragment of the IAP gene (see Fig. 1) also inserted into M13. In this case an upstream 15-nucleotide primer (P-L Biochemicals) was used for duplex synthesis. The double-stranded insert was excised with *Bam*HI, the strands were separated (36), and the self-hybridizing fraction of the tracer was removed by hydroxyapatite chromatography (37).

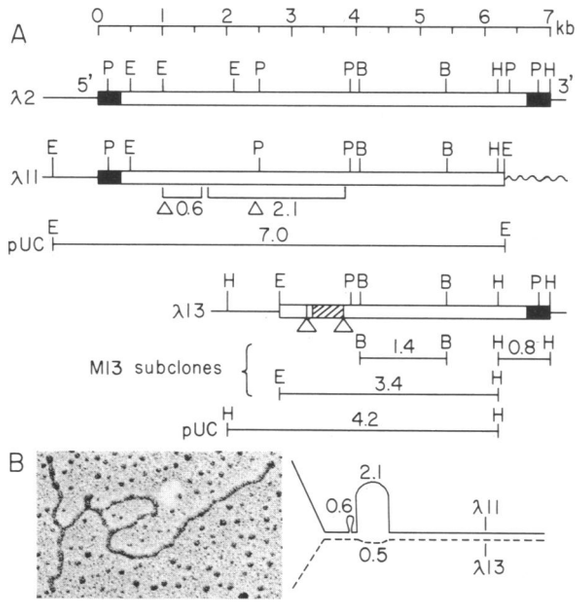

FIG. 1. Structure of three IAP genes carried in different λ phage Charon 4A clones, 2, 11, and 13. (*A*) Restriction enzyme maps of the three genes with respect to some conserved restriction sites: E, *Eco*RI; H, *Hin*dIII; B, *Bam*HI; P, *Pst* I. ■, LTR of about 0.35 kb (20, 21); —, flanking mouse sequences; and ∿∿∿, λ phage sequences. In clone 11, brackets indicate the locations of two segments, Δ 0.6 and Δ 2.1, which are deleted in clone 13; in the latter clone, an inserted segment (▨) of about 0.5 kb is indicated. Under the diagrams of clones 11 and 13 are shown the locations and sizes in kb of fragments subcloned in the plasmid pUC8 and the single-stranded DNA phage M13mp8 for use as hybridization probes or for heteroduplex analysis. (*B*) Electron micrograph and diagrammatic representation of a heteroduplex between the 7-kb *Eco*RI (partial digestion) fragment of clone 11 and the 4.2-kb *Hin*dIII fragment of clone 13 in *A*; both fragments were subcloned in pUC8 and excised with *Hin*dIII (for the 7-kb fragment using the *Hin*dIII site at the 3′ end and the *Hin*dIII site of the pUC8 cloning sequence located at the 5′ end of the fragment). The diagram depicts the origin and size in kb of the mismatched segments.

Assay of RNA by Dot Hybridization. Unlabeled embryo RNA and myeloma RNA standard were denatured by heating in 0.02 M sodium phosphate, pH 7/1 mM EDTA/2.2 M formaldehyde/50% formamide (deionized) at 60°C for 5 min, brought to 20× standard saline citrate (1× is 0.15 M NaCl/0.015 M Na citrate) in a volume of 150–200 μl, and dotted onto a nitrocellulose sheet (BA85, Schleicher & Schuell) in a Hybridot apparatus (Bethesda Research Laboratories). The filters were baked at 80°C for 2 hr in a vacuum oven; prehybridized for 3 hr at 42°C in 1 M NaCl/50 mM sodium phosphate, pH 7, containing 0.02% each of bovine serum albumin, Ficoll, and polyvinylpyrrolidone, 0.1% $NaDodSO_4$, 4 mM EDTA, 50% (vol/vol) formamide, and 100 μg of sonicated denatured calf thymus DNA per ml; and hybridized in the same buffer with $1\text{–}2 \times 10^7$ cpm of ^{32}P-labeled DNA probe per ml for 20 hr at 42°C. The filters were washed with vigorous shaking three times for 5 min at 25°C and six times for 20 min at 68°C in 0.25 M NaCl/12.5 mM sodium phosphate, pH 7/1 mM EDTA/0.1% $NaDodSO_4$, dried, and autoradiographed for 1–4 days at −70°C on preflashed x-ray films with intensifying screens.

Hybridization of Labeled RNA to Filter-Bound DNA. Recombinant DNA samples were denatured and dotted onto nitrocellulose filters (2 μg of DNA per dot) in the Hybridot apparatus as described above and were hybridized with labeled embryo RNA for 20 hr at 68°C in 50 μl of 0.6 M NaCl/0.12 M Tris·HCl, pH 7.5/4 mM EDTA/0.2% $NaDodSO_4$/1 mg of *E. coli* tRNA per ml in siliconized plastic tubes under mineral oil. Filter-bound λ phage DNA was included in each sample for background correction. After hybridization, the filters were washed three times for 5 min at 25°C and six times for 20 min at 68°C in 0.15 M NaCl/30 mM Tris·HCl, pH 7.5/1 mM EDTA/0.1% $NaDodSO_4$, air-dried, and counted in 2,5-diphenyloxazole/toluene. The data were corrected for efficiency of hybridization (40–60%) determined in parallel samples from the binding of ^{3}H-labeled λ phage cRNA to λ phage DNA.

RESULTS

Recombinant DNA Clones. Fig. 1*A* shows the restriction enzyme maps of three IAP genes selected from the mouse genomic library and used in the present study. Clone 2 contained a complete IAP gene, ≈7 kb in size including the two LTRs. The IAP gene in clone 11 was truncated at its 3′ end, abutting λ phage sequences, but formed a well-matched heteroduplex over its 6.3-kb length with the IAP gene in clone 2 (not shown). The two genes also had identical restriction sites with three of the enzymes tested but varied in *Eco*RI sites. These genes are clearly representative of the predominant 7-kb IAP gene described previously (17–19). The IAP gene in clone 13 is flanked by mouse DNA sequences, but its 5′ end is truncated at an *Eco*RI site, presumably due to accidental recombination at this site during construction of the clones. Heteroduplex analysis between this clone and clone 11 revealed deletions of about 2.1 and 0.6 kb as well as an inserted segment of about 0.5 kb in clone 13 (Fig. 1*B*); this sequence organization appears to be representative of a subfamily of IAP genes, designated type II genes by Shen-Ong and Cole (17). Of the 10 IAP genomic clones analyzed by us, 6 contained typical 7-kb genes (or segments thereof), 2 contained type II genes, and 2 contained genes with deletions of about 0.6 and 3.7 kb, the latter being similar in sequence organization to the *81-B* gene of Cole *et al.* (38).

Detection of IAP RNA in Embryos by Dot Hybridization. Total embryo RNA (treated with DNase) was dotted onto nitrocellulose filters and hybridized with ^{32}P-labeled M13 DNA containing IAP gene sequences. A 1:1 serial dilution of an RNA preparation from the myeloma MOPC-104E was

also dotted in each experiment as a standard of comparison. The content of IAP RNA in the standard was determined by titration against the ^{32}P-labeled template strand of the 1.4-kb *Bam*HI fragment from clone 13. From the slope of the titration curve, an IAP RNA content of 2.13×10^5 molecules per ng of total RNA was derived (Fig. 2).

IAP-related RNA sequences were detected in both ovarian oocytes and early embryos, but the intensity of hybridization varied widely depending on the stage of development (Fig. 3 *A* and *B*). When RNA from a constant number of embryos (50 embryos each) was dotted (Fig. 3*A*), mid-size and fully grown oocytes reacted strongly, but the reaction of ovulated unfertilized eggs was barely detectable; the reaction of two-cell embryos was several-fold stronger, and the intensity of the reaction continued to increase during cleavage to a high level in the preimplantation (4-day-old) blastocyst. Although most of the dot hybridizations were performed with the 0.8-kb *Hin*dIII fragment (which includes the 3′ LTR) as a probe, an identical pattern of reactivity was obtained with the 1.4-kb *Bam*HI and the 3.4-kb *Eco*RI–*Hin*dIII fragments, which lack LTR sequences (data not shown). Control hybridizations with labeled M13 DNA containing the nontranscribed strand of these fragments were completely negative, indicating that the above reactions were due to the presence of RNA sequences in the embryos rather than to contaminating nuclear DNA. On the basis of densitometric tracings of the autoradiographs, we estimated the number of IAP-related RNA molecules per embryo in relation to the myeloma RNA standard (Table 1), assuming that the number of reactive sites per molecule is the same in the two preparations (presumably both ends of an RNA transcript when hybridized with the 0.8-kb *Hin*dIII probe containing LTR sequences).

To estimate how much of the IAP RNA is polyadenylylated, total RNA from early and late blastocysts was fractionated on poly(U)-Sepharose (28), and the bound and unbound fractions were dotted and hybridized with the 0.8-kb *Hin*dIII probe. About 60% of the total reactive RNA was in the bound fraction in each sample, suggesting that the majority of the IAP RNA in the embryos is polyadenylylated but a substantial fraction lacks poly(A) sequences (data not shown).

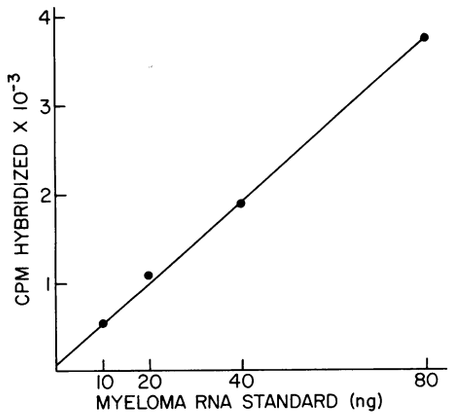

FIG. 2. Titration of single-stranded 1.4-kb *Bam*HI fragment with a standard RNA preparation (treated with DNase) from myeloma MOPC-104E. Increasing RNA concentrations were incubated for 44 hr with 50 pg of ^{32}P-labeled probe DNA (specific activity, 3.0×10^8 cpm/μg) in 10 μl of 1.0 M NaCl/50 mM Tris·HCl, pH 7.5/5 mM EDTA/0.1% $NaDodSO_4$ with 1 mg of *E. coli* tRNA per ml in sealed glass capillary tubes (DNA C_0t = 8 times $C_0t_{1/2}$ for the probe). Hybrid formation was assayed by S1 nuclease digestion and collection of the resistant material on DE81 filters for counting. The specific activity of the probe was monitored by titration with known amounts of the complementary strand. In two experiments, the average number (±SD) of IAP RNA molecules per ng of myeloma RNA was $2.13 \pm 0.09 \times 10^5$.

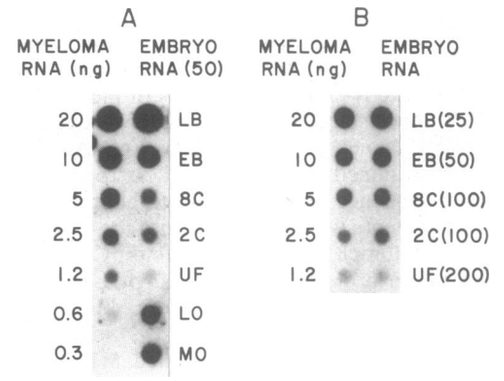

FIG. 3. Autoradiographs showing the hybridization of RNA dots from mouse oocytes and embryos with labeled cloned DNA. All RNA preparations used for dotting were treated with DNase. (*A*) Total RNA derived from 50 oocytes and embryos was dotted onto a nitrocellulose filter, hybridized with ^{32}P-labeled M13 phage DNA containing the 0.8-kb *Hin*dIII fragment of clone 13, and autoradiographed. A 1:1 dilution series of myeloma MOPC-104E RNA was dotted on the same filter as a standard of comparison. (*B*) The same experiment as above, but the amount of embryo RNA was varied so as to bring the intensity of the reaction within the range of the standard RNA; the number of embryos used is shown in parenthesis. Stages of embryo development: MO, mid-size oocyte 50–55 μm in diameter recovered from 9-day-old mice; LO, large fully grown oocyte ≈70 μm in diameter obtained from 15-day-old mice; UF, unfertilized tubal egg; 2c, two-cell embryo; 8c, eight-cell embryo; EB, early blastocyst (32 cells); LB, late blastocyst (64 cells). The chronological age of the embryos is given in Table 1.

Size of IAP RNA. The size of the IAP RNA in late blastocysts was estimated by electrophoresis on a formaldehyde-agarose gel and blot hybridization with ^{32}P-labeled cloned DNA probes (Fig. 4). A single reactive band was observed with an estimated size of ≈5.4 kb. The reactive material on the top of the lane is assumed to be nuclear DNA; this material was absent when the RNA sample was precipitated with 2 M LiCl, which does not precipitate DNA (28).

Synthesis of IAP RNA in Early Embryos. To obtain information on the overall rates of IAP RNA synthesis, we labeled mouse embryos *in vitro* with [^{3}H]adenosine and assayed the amounts of labeled IAP-related RNA sequences

Table 1. Amounts of IAP-related RNA in oocytes and early embryos

Hours after HCG injection*	Stage of development	IAP-related RNA per embryo: No. of molecules $\times 10^{-3}$†	IAP-related RNA per embryo: Mass, fg‡
—	Mid-size oocyte	20.3	61
—	Fully grown oocyte	17.0 ± 1.0	51
24	Unfertilized egg	1.3 ± 0.3	4
53	Late two-cell	7.1 ± 0.4	21
72	Eight-cell	9.7 ± 0.2	29
96	Early blastocyst	37.9 ± 7.9	115
120	Late blastocyst	156.0 ± 33.0	472

*Approximate age of embryos used for RNA extraction. Ovulation occurs at 12–14 hr, first cleavage at 31–33 hr, and second cleavage at 53–55 hr after the injection of human chorionic gonadotropin (HCG).

†Calculated from densitometric tracings of autoradiographs obtained in dot-hybridization experiments as shown in Fig. 3 by using a concentration of 2.13×10^5 IAP RNA molecules per ng of total RNA in the RNA standard. The autoradiographs were exposed for different times so as to bring the density of the experimental dots within the linear range of the tracings of the standard RNA. The mean ± SEM for three experiments is given except for the value for mid-size oocytes, which was obtained in a single experiment.

‡Calculated by using a molecular mass of 1.8×10^6 daltons.

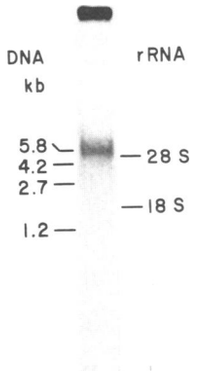

FIG. 4. Blot hybridization of RNA from mouse blastocysts with ^{32}P-labeled cloned DNA. A total nucleic acid extract from 200 expanded (4-day-old) blastocysts was electrophoresed on a 1% agarose/2.2 M formaldehyde slab gel (39), blotted onto a nitrocellulose filter in 20× standard saline citrate for 18 hr, and hybridized as described for dot hybridization. The labeled probe (a total of 4×10^7 cpm/ml) was an equimolar mixture of the 0.8-kb *Hin*dIII and 1.4-kb *Bam*HI fragments carried in M13 phage DNA which was ^{32}P-labeled by partial duplex synthesis to a specific activity of 2×10^8 cpm/μg. Autoradiography was for 16 hr. The marker DNAs were IAP gene restriction fragments and 2.7-kb linear pUC8 DNA, which were run on a parallel lane and were blotted and hybridized together with the embryo RNA. The location of the 18 and 28S rRNAs was determined from 0.6 μg of myeloma RNA run on a parallel lane and stained with ethidium bromide.

by hybridization to filter-bound cloned IAP genes. The synthesis of IAP RNA was detected between the two-cell stage and the late blastocyst, and the rate of synthesis per embryo increased about 30-fold during this period (Table 2). This increase appears to be due almost entirely to an increase in cell number per embryo, as the rate of synthesis per cell remained about the same, ≈4 fg over a 5-hr period, at all the stages examined. The same rate of hybridization was obtained whether total clone 2 DNA or the 7-kb *Eco*RI fragment of clone 11 inserted in pUC8 was used as a probe, thus ruling out the possibility that flanking mouse DNA rather than IAP gene sequences are involved. Some synthesis of IAP RNA appeared to take place also in late one-cell embryos, but the level of radioactivity hybridized was too low to assess the rate of synthesis (data not shown). Thermal melts of hybrids between labeled embryo RNA and IAP genes indicated a sharp transition, with a t_m about 3°C below that of hybrids between λ phage [^{3}H]cRNA and λ phage DNA, suggesting a good match between the embryo IAP RNA and IAP gene sequences (Fig. 5).

DISCUSSION

The results of this study show the presence of IAP-related RNA sequences in mouse oocytes and early embryos. Most of the IAP RNA isolated from blastocysts consisted of a single size class of ≈5.4 kb, and a major fraction of this RNA (≈60%) was polyadenylylated. IAP RNA species isolated from mouse tumor cells fall into several discrete size classes of 3.5–7 kb (14, 15, 17), and there is some evidence suggesting that the size variability is due to the transcription of different sets of genes rather than to differential processing of the RNA transcripts (17). If this is the case, then the IAP RNA of early embryos may be the product of a deletion variant of the predominant 7-kb gene.

Dot hybridization experiments revealed a marked variation in the amounts of IAP RNA at different stages of development. IAP RNA was relatively abundant in growing and fully grown oocytes, decreased to ≈1/10th in the ovulated egg, and increased by ≈100-fold between the one-cell and late blastocyst stages (Fig. 3 and Table 1). The change in abundance of IAP RNA during this period is quantitatively more pronounced than that observed for total poly(A)$^+$ RNA and also differs from the latter in its timing, inasmuch as most of the maternal IAP RNA appears to have been eliminated in the ovulated egg, whereas the bulk (≈70%) of the

Table 2. Rate of synthesis of IAP RNA in early mouse embryos

Stage of development*	Adenosine incorporated, fmol/5 hr per embryo		IAP RNA synthesized,† fg/5 hr per	
	Total RNA	IAP RNA ± SEM	Embryo	Cell
Late two-cell	12.7	0.007 ± 0.002	7.8	3.9
Eight- to 16-cell	104.2	0.038 ± 0.006	42.1	3.5
Early blastocyst	296.7	0.143 ± 0.011	156.9	4.9
Late blastocyst	329.2	0.230 ± 0.007	251.0	3.9

Batches of 200–600 embryos were incubated for 5 hr in the presence of 50 μM [2,8-^{3}H]adenosine (42 Ci/mmol; 1 Ci = 37 GBq). Total adenosine incorporation per embryo was calculated from the total acid-precipitable radioactivity in a sample of 3–6 embryos and the specific activity of the ATP pool (ranging from 25% to 45%) at the termination of labeling. Pool specific activity was derived from the total soluble radioactivity contained in a parallel sample of embryos (assuming that 90% of this label was converted into ATP) and the known size of the endogenous ATP pool (28, 40); for blastocysts, this value was corrected for the estimated [^{3}H]ATP content of the blastocele fluid (40). The values of adenosine incorporation represent the average of 2–4 determinations. More than 90% of the acid precipitable radioactivity was sensitive to digestion with alkali or RNase A/T1 in low-salt buffer. The total labeled embryo RNA was extracted, treated with DNase I, and hybridized to filter-bound cloned IAP DNA (total clone 2 DNA or the 7-kb *Eco*RI fragment of clone 11, subcloned in pUC8 as shown in Fig. 1; 4 μg of DNA per sample). Adenosine incorporation into IAP RNA per embryo was calculated from the fraction of ^{3}H label in hybrid form in relation to the total acid-precipitable radioactivity in the hybridization mixture and the rate of adenosine incorporation per embryo determined as described above. The values are corrected to an efficiency of hybridization of 100%.

*The chronological age of embryos at the beginning of radioisotope labeling was the same as in Table 1 except that two-cell embryos were set up for labeling 48 hr after injection of human chorionic gonadotropin.

†The amount of IAP RNA was calculated on the basis of an A+T content of 60 mol% for the IAP genome (19). For 8- to 16-cell embryos, an average cell number of 12 was used.

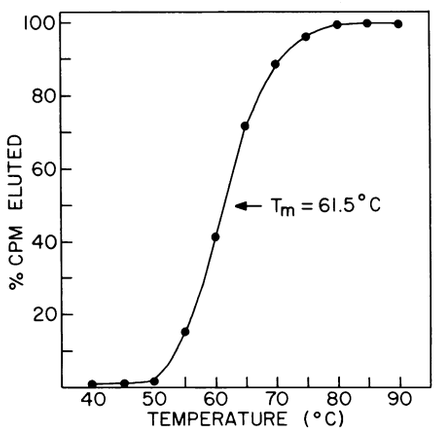

FIG. 5. Thermal melt of hybrids formed between ^{3}H-labeled embryo RNA and IAP gene sequences. Eight-cell embryos were labeled with [^{3}H]adenosine for 5 hr, and the total RNA was extracted, treated with DNase I, and hybridized to filter-bound clone 2 DNA as described in Table 2. Thermal elution of RNA was carried out as described by Childs *et al.* (41). After scintillation counting, the filters were washed three times with chloroform, dried, and suspended in 0.1× standard saline citrate. The temperature was raised in 5°C increments, and the eluted RNA was removed and assayed for radioactivity. The total eluted radioactivity was 400 cpm. In the same conditions, hybrids between λ phage [^{3}H]cRNA and λ phage DNA melted with a t_m of 65°C.

maternal poly(A)$^+$ RNA is lost at the two-cell stage (23, 25). New synthesis of IAP RNA occurs from the two-cell stage onwards at an approximately constant rate per cell (≈4 fg per cell over a 5-hr period; Table 2) and accounts for the steep rise in IAP RNA content by the blastocyst stage. The mass of IAP RNA is 0.25–0.5% of the estimated poly(A)$^+$ RNA content in cleavage-stage embryos (25).

It is interesting to compare the number of IAP RNA molecules derived in the present study with the pattern of expression of morphologically detectable particles in oocytes and early embryos. Although no direct information is available on A-type particle expression in the $CD2F_1$ mice used by us, the general pattern of particle expression has been similar in >12 mouse strains that have been examined, and the $CD2F_1$ mice may be expected to resemble the maternal BALB/c strain, which has been studied in detail (3–7). A qualitative correlation appears to exist between the presence of IAP predominantly in oocytes up to the time of ovulation and in embryos from the 8- to 16-cell stage onwards, on the one hand, and the relative abundance of IAP RNA, on the other. However, even in oocytes and morula-blastocyst stage embryos, the number of IAPs amounts to only a few particles per equatorial section—on the order of 1,000 particles per embryo (refs. 3 and 4; unpublished data), which is 1/30th to 1/100th the number of IAP RNA molecules at these stages (Table 1). Therefore, in contrast to tumor (myeloma) cells, where most of the IAP RNA is associated with particles (27), nearly all the IAP RNA in embryo cells occurs in a form not bound to particles and, thus, is potentially available for protein synthesis. However, the distribution of IAP RNA between the nucleus and cytoplasm of embryonic cells remains to be determined.

A comparison of the number of IAP RNA molecules with the expression of IAP(ε) or "small A" particles in early embryos reveals a striking discrepancy. Not only is there no correlation between the pattern of expression of IAP(ε) and the relative abundance of IAP RNA, but the massive budding of IAP(ε) in two-cell embryos, $\approx 1\text{–}2 \times 10^5$ particles per embryo in an average particle-producing strain such as BALB/c (refs. 3 and 4; unpublished data), occurs at a time when IAP RNA is relatively sparse, $<10^4$ molecules per embryo (Table 1). This large quantitative difference suggests that IAP(ε) is genetically distinct from IAP and presumably represents another family of endogenous retroviral genes. A possible antigenic relationship between IAP(ε) and IAP has been suggested by an immuno-electron-microscopic study in which treatment with anti-IAP antiserum produced a diffuse staining of endoplasmic reticulum cisternae containing budding IAP(ε) (10); however, it is not clear in this study whether the reaction is due to an antigen associated with the IAP(ε) particles themselves or some other antigen that is secreted into the cisternae.

Immunological studies suggest that the IAP RNA of early mouse embryos is active in protein synthesis. Antibody against IAP from mouse myeloma precipitated a set of five proteins with M_rs of 67,000–77,000 synthesized in two- to eight-cell embryos; two of these proteins with M_rs of 75,000 and 77,000 were synthesized also in morulae and blastocysts (42). The relationship between the five protein species—namely, whether they represent modified forms of the same precursor—is not known. IAP-related antigen(s) have been detected on the cell surface from the zygote to the eight-cell stage (9, 10), but the functional significance of this finding is unclear. Nevertheless, the lack of association of most of the IAP RNA with particles, the variability of form of IAP-related antigens, and the occurrence of these antigens on the cell surface suggest that the control of expression of IAP gene(s) in embryos is different from that occurring in tumor cells.

We thank Mary Ann Chie for excellent technical assistance. We are indebted to Mark Davis for his help in screening the mouse genomic library. This work was supported by the Medical Research Service of the Veterans Administration and by U.S. Public Health Service Grant CA24989 from the National Cancer Institute.

1. Pikó, L. (1975) in *The Early Development of Mammals*, eds. Balls, M. & Wild, A. E. (Cambridge Univ. Press, Cambridge), pp. 167–187.
2. Kelly, F. & Condamine, H. (1982) *Biochim. Biophys. Acta* **651**, 105–141.
3. Chase, D. & Pikó, L. (1973) *J. Natl. Cancer Inst.* **51**, 1971–1975.
4. Yotsuyanagi, Y. & Szollosi, D. (1981) *J. Natl. Cancer Inst.* **67**, 677–685.
5. Calarco, P. G. & Brown, E. H. (1969) *J. Exp. Zool.* **171**, 253–284.
6. Calarco, P. G. & Szollosi, D. (1973) *Nature (London) New Biol.* **243**, 91–93.
7. Biczysko, W., Pienkowski, M., Solter, D. & Koprowski, H. (1973) *J. Natl. Cancer Inst.* **51**, 1041–1050.
8. Kuff, E. L., Lueders, K. K., Ozer, H. L. & Wivel, N. A. (1972) *Proc. Natl. Acad. Sci. USA* **69**, 218–222.
9. Huang, T. T. F., Jr., & Calarco, P. G. (1981) *Dev. Biol.* **82**, 388–392.
10. Huang, T. T. F., Jr., & Calarco, P. G. (1982) *J. Natl. Cancer Inst.* **68**, 643–649.
11. Lueders, K. K. & Kuff, E. L. (1979) *J. Virol.* **30**, 225–231.
12. Callahan, R., Kuff, E. L., Lueders, K. K. & Birkenmeier, E. (1981) *J. Virol.* **40**, 901–911.
13. Wilson, S. H. & Kuff, E. L. (1972) *Proc. Natl. Acad. Sci. USA* **69**, 1531–1536.
14. Paterson, B. M., Segal, S., Lueders, K. K. & Kuff, E. L. (1978) *J. Virol.* **27**, 118–126.
15. Ono, M., Cole, M. D., White, A. T. & Huang, R. C. C. (1980) *Cell* **21**, 465–473.
16. Lueders, K. K. & Kuff, E. L. (1977) *Cell* **12**, 963–972.
17. Shen-Ong, G. L. C. & Cole, M. D. (1982) *J. Virol.* **42**, 411–421.
18. Lueders, K. K. & Kuff, E. L. (1980) *Proc. Natl. Acad. Sci. USA* **77**, 3571–3575.
19. Kuff, E. L., Smith, L. A. & Lueders, K. K. (1981) *Mol. Cell. Biol.* **1**, 216–227.
20. Cole, M. D., Ono, M. & Huang, R. C. C. (1981) *J. Virol.* **38**, 680–687.
21. Kuff, E. L., Feenstra, A., Lueders, K., Smith, L., Hawley, R., Hozumi, N. & Shulman, M. (1983) *Proc. Natl. Acad. Sci. USA* **80**, 1992–1996.
22. Kuff, E. L., Feenstra, A., Lueders, K., Rechavi, G., Givol, D. & Canaani, E. (1983) *Nature (London)* **302**, 547–548.
23. Pikó, L. & Clegg, K. B. (1982) *Dev. Biol.* **89**, 362–378.
24. Eppig, J. J. (1976) *J. Exp. Zool.* **198**, 375–382.
25. Clegg, K. B. & Pikó, L. (1983) *Dev. Biol.* **95**, 331–341.
26. Wensink, P. C., Finnegan, D. J., Donelson, J. E. & Hogness, D. S. (1974) *Cell* **3**, 315–325.
27. Lueders, K. K., Segal, S. & Kuff, E. L. (1977) *Cell* **11**, 83–94.
28. Clegg, K. B. & Pikó, L. (1982) *Nature (London)* **295**, 342–345.
29. Davis, M. M., Calame, K., Early, P. W., Livant, D. L., Joho, R., Weissman, I. L. & Hood, L. (1980) *Nature (London)* **283**, 733–739.
30. Benton, W. D. & Davis, R. W. (1977) *Science* **196**, 180–182.
31. Southern, E. (1979) *Methods Enzymol.* **68**, 152–176.
32. Messing, J. & Vieira, J. (1982) *Gene* **19**, 269–276.
33. Vieira, J. & Messing, J. (1982) *Gene* **19**, 259–268.
34. Howarth, A. J., Gardner, R. C., Messing, J. & Shepherd, R. J. (1981) *Virology* **112**, 678–685.
35. Hu, N.-T. & Messing, J. (1982) *Gene* **17**, 271–277.
36. Maxam, A. M. & Gilbert, W. (1980) *Methods Enzymol.* **65**, 449–560.
37. Britten, R. J., Graham, D. E. & Neufeld, B. R. (1974) *Methods Enzymol.* **29**, Part E, 363–406.
38. Cole, M. D., Ono, M. & Huang, R. C. C. (1982) *J. Virol.* **42**, 123–130.
39. Lehrach, H., Diamond, D., Wozney, J. M. & Boedtker, H. (1977) *Biochemistry* **16**, 4743–4751.
40. Clegg, K. B. & Pikó, L. (1977) *Dev. Biol.* **58**, 76–95.
41. Childs, G., Maxson, R. & Kedes, L. H. (1979) *Dev. Biol.* **73**, 153–173.
42. Huang, T. T. F., Jr., & Calarco, P. G. (1981) *J. Natl. Cancer Inst.* **67**, 1129–1134.